Aquatic transport

- Konzeptuelle Modelle

- Spezifische Aktivitäten in Abhängigkeit von der Korngröße

- Verteilung von RN im Sediment / Tiefenprofile

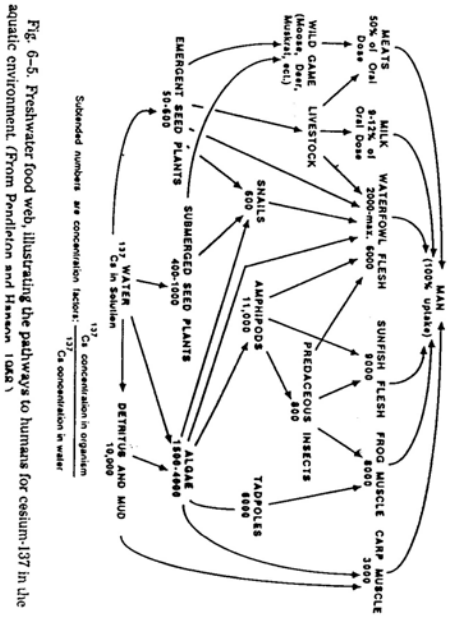

Fig. 6–5. Freshwater food web, illustrating the pathways to humans for cesium-137 in the aquatic environment. (From Pendleton and Hanson, 1968.)

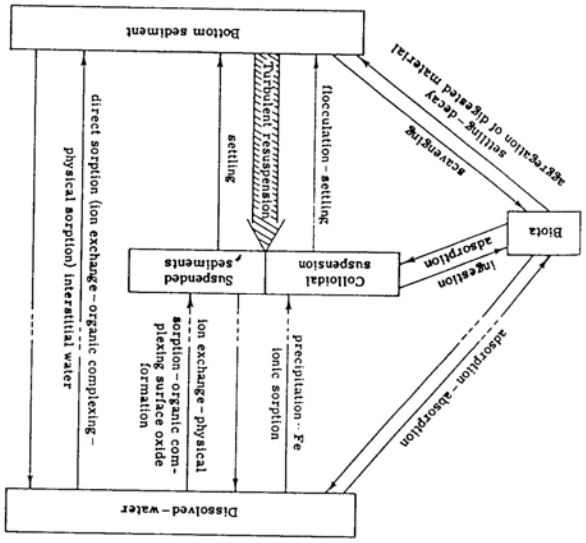

Fig. 6–6. Basic components of the aquatic ecosystem. The complexities of the pathways among the biota are illustrated in Fig. 6–5. (From Hair, 1974.)

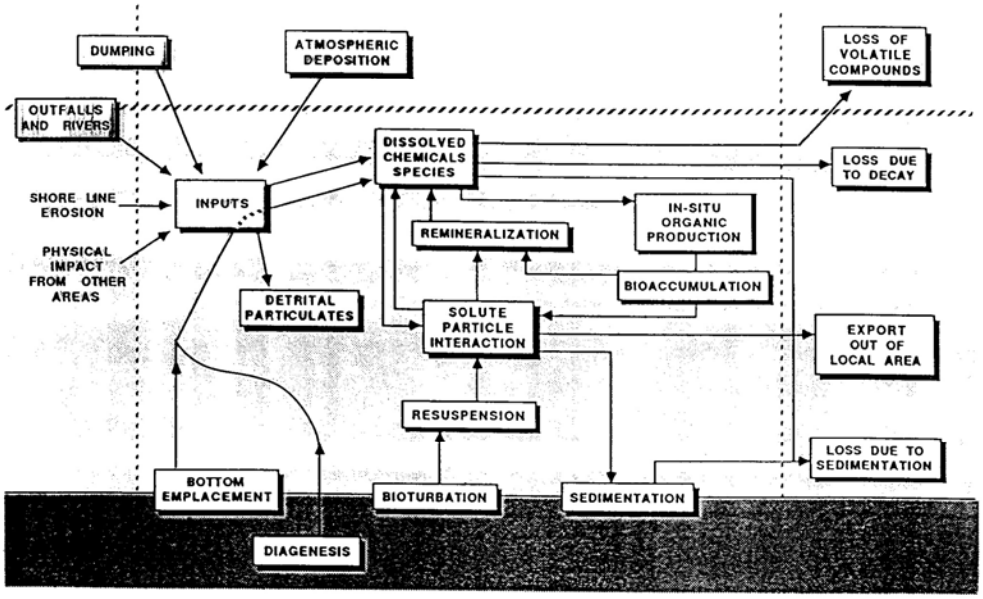

Fig. 6–14. Possible transformations of a pollutant in the water column. (From National Oceanic and Atmospheric Administration, 1979.)

Table 4.23 Concentration ratio (CR) for ^{137}Cs, ^{90}Sr, $^{239,240}Pu$ and ^{241}Am at Bikini Island for several species of vegetation. Mean (median) CR (Bq per g in fruit, wet weight/Bq/g in 0–40 cm soil, dry weight)

	^{137}Cs	^{90}Sr	$^{239,240}Pu$	^{241}Am
Drinking coconut meat	5.5 (3.4)	6.1×10^{-3} (4.5×10^{-3})	2.8×10^{-5} (7.1×10^{-6})	5.3×10^{-5} (1.4×10^{-5})
Drinking coconut fluid	2.1 (1.3)	—	—	—
Copra meat	10 (4.2)	4.6×10^{-3} (3.1×10^{-3})	1.9×10^{-5} (6.0×10^{-6})	3.1×10^{-5} (8.2×10^{-6})
Breadfruit	0.8 (0.6)	0.057 (0.055)	1.3×10^{-5} (4.2×10^{-6})	2.4×10^{-5} (6.5×10^{-6})
Pandanus	15 (11)	0.12 (0.041)	2.3×10^{-5} (1.3×10^{-5})	6.3×10^{-5} (3.0×10^{-5})

Table 5.1 A comparison of K_d values[a] in freshwater and seawater

Element	Freshwater	Seawater
I	3×10^2	10^1
Na	10^2	10^1
Ru	10^2	5×10^3
Sr	10^3	10^2
Cs	10^4	2×10^3
Pu	10^5	5×10^4
Lanthanides	5×10^6	5×10^5

[a] Values are the best estimates from Coughtrey *et al.* (1985).

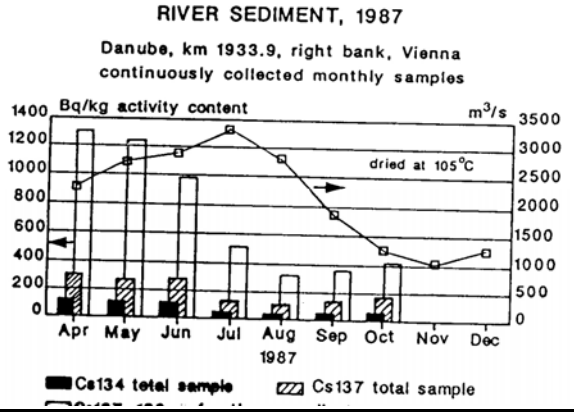

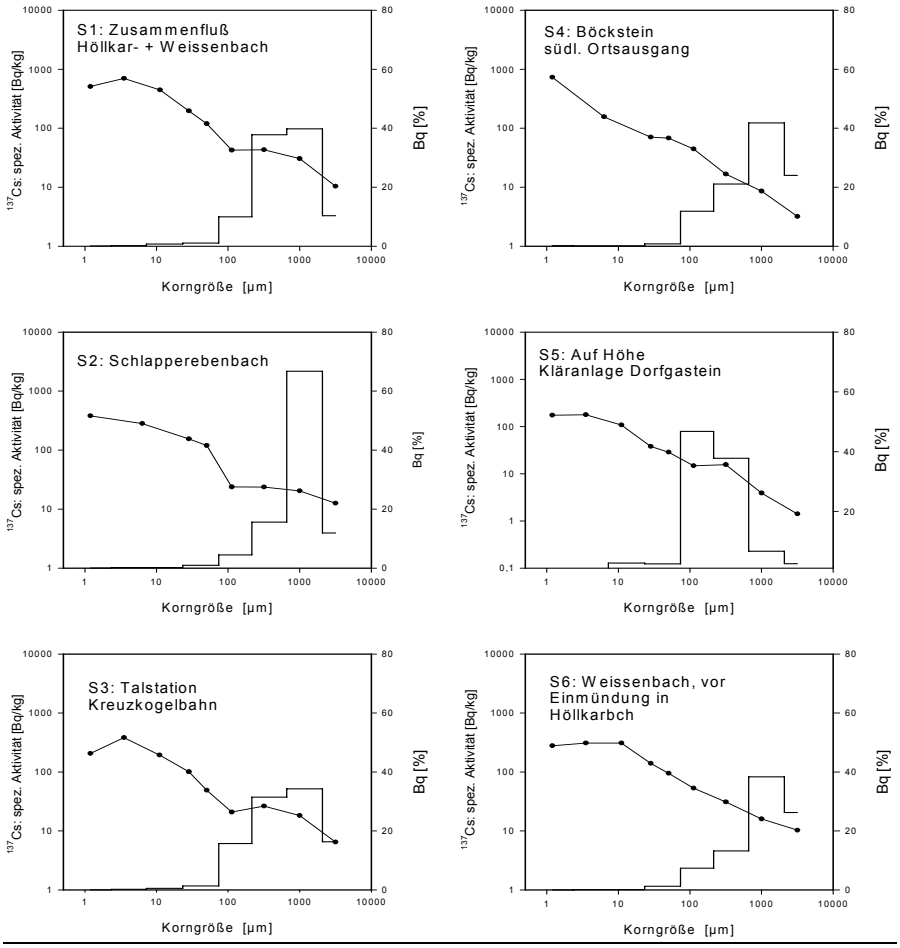

Spezifische Aktivität in Abhängigkeit von der Korngrößenklasse (Linie mit vollen Kreisen) und prozentueller Anteil an der Gesamtaktivität [Stufenfunktion). Bezugszeit: 1.1.2001

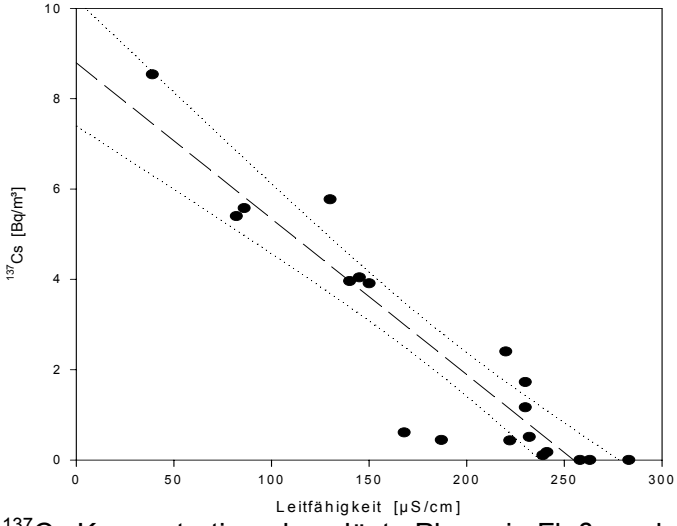

^{137}Cs Konzentration als gelöste Phase in Fluß- und Bachwasser und Abhängigkeit von der Leitfähigkeit

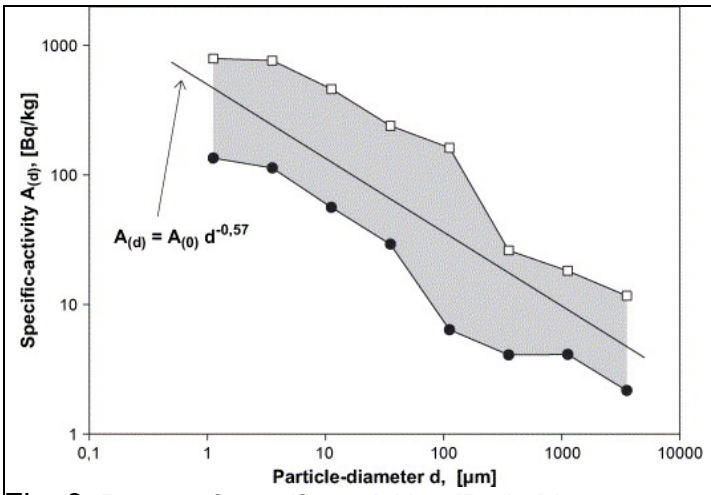

Fig. 3. Range of specific activities [Bq/kg] in sediments depending on particle diameter [µm], expressed as geometric mean of a particle size class. Straight line, resp. power function based on arithmetic mean for k_2 (see text).

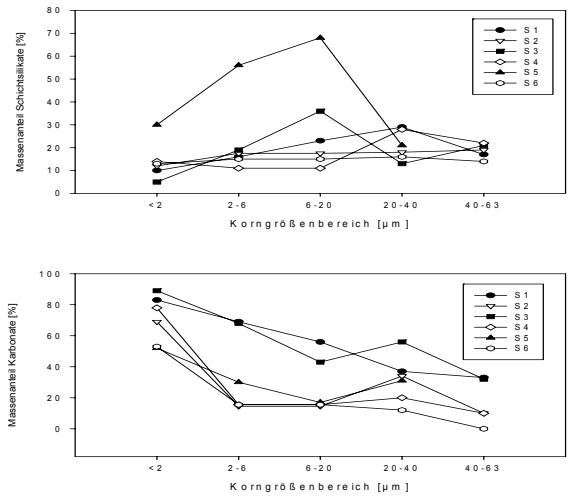

Zusammenhang zwischen den Massenanteilen an Karbonaten (Kalzit + Dolomit + Aragonit), sowie Schichtsilikaten (Chlorit, Muskovit, Biotit) und dem Korngrößenbereich.

$$A_{geo} = \frac{1}{\rho} k_1 r^{k_2 - 3}$$

k_2

„Shape" Parameter, Can be defined as **fractal dimension**

k_2 = 2 for euclidian geometry

k_2 = 3; dimension of volume
SSA no longer depends on r !
⇒ Pores fill total volume !

k_2 = 2,65; significant contribution of volume

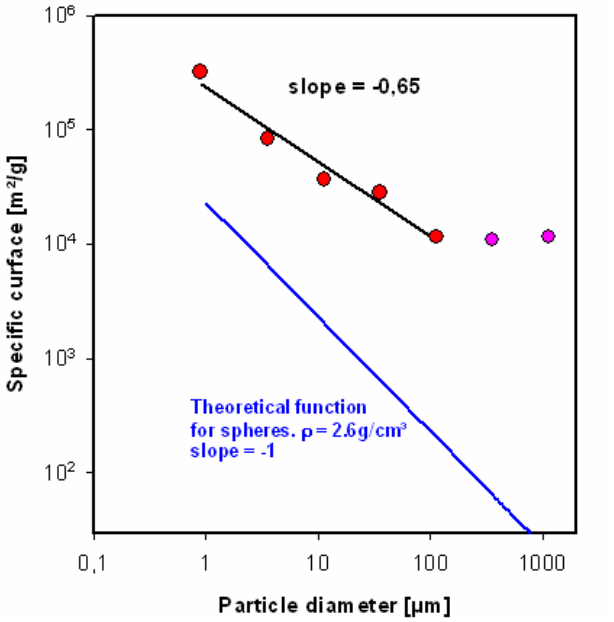

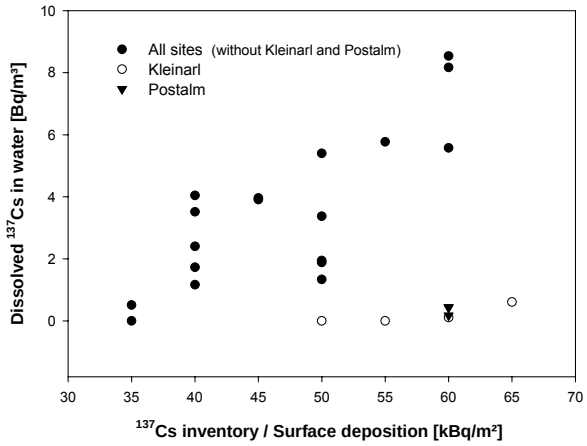

Concentration of dissolved ^{137}Cs [Bq/m³] in water vs. surface deposition [kBq/m²] of the drained catchment

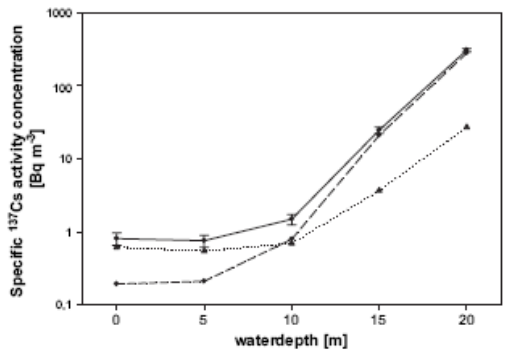

Vertical depth distribution of ^{137}Cs in water samples of Lake Wallersee.

Radionuklidprofile für ^{137}Cs und ^{210}Pb in Seesedimenten aus dem Wallersee

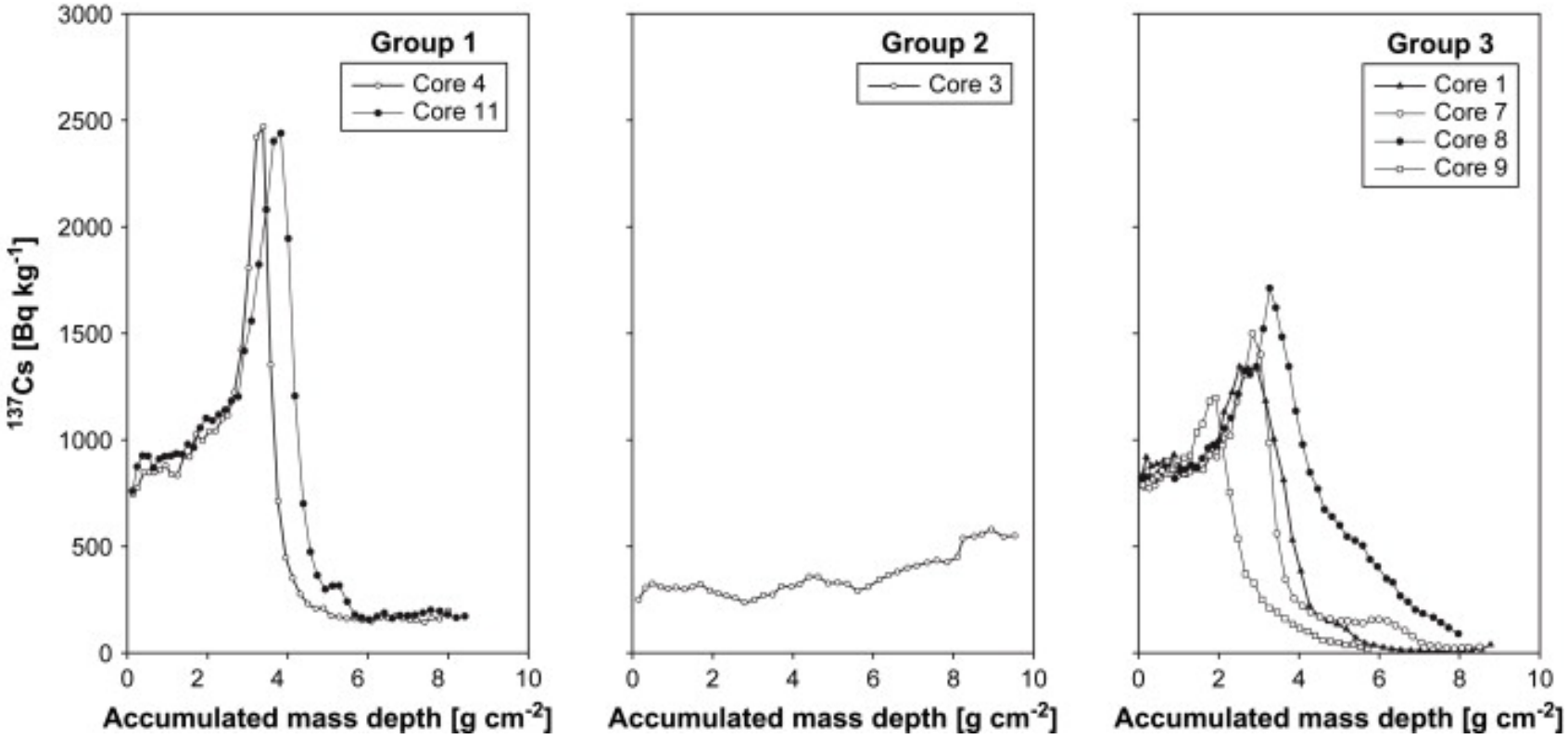

Fig. 3. ^{137}Cs activity profiles in selected sediment cores from maximum depth (group (1): cores 4 and 11), debris fan in maximum depth (group (2): core 3) and from intermediate lake depths (group (3): cores 1, 7–9). t_o: 29th July 2004. (J.Env.Rad. 99/8, 2008)

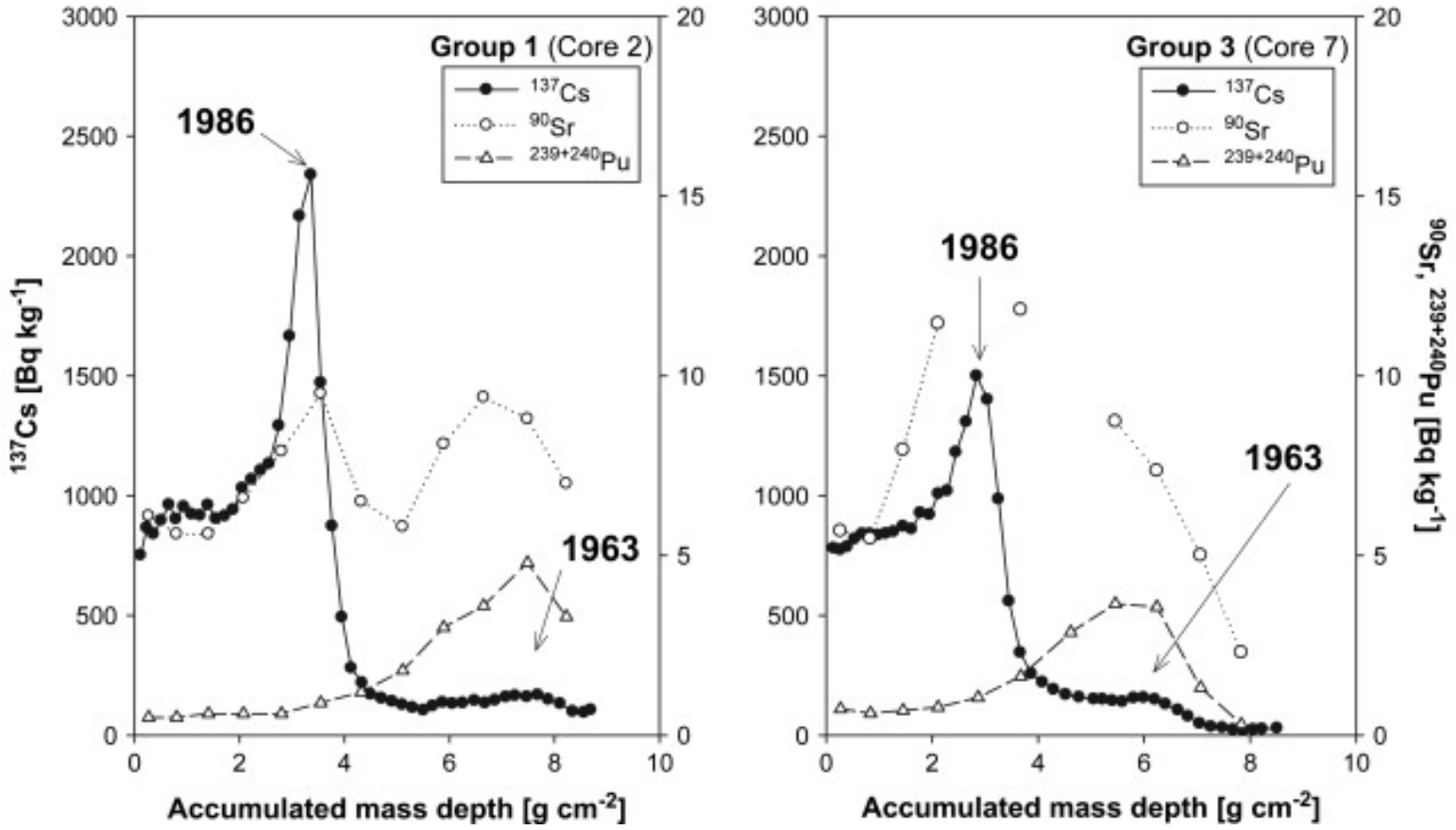

Fig. 4. Activity profiles of ^{90}Sr, $^{239+240}$Pu, and ^{137}Cs exemplarily shown in a core from groups (1) and (3). Uncertainties for ^{90}Sr and $^{239+240}$Pu is <15% for ^{137}Cs < 5%. t_o: 29th July 2004.

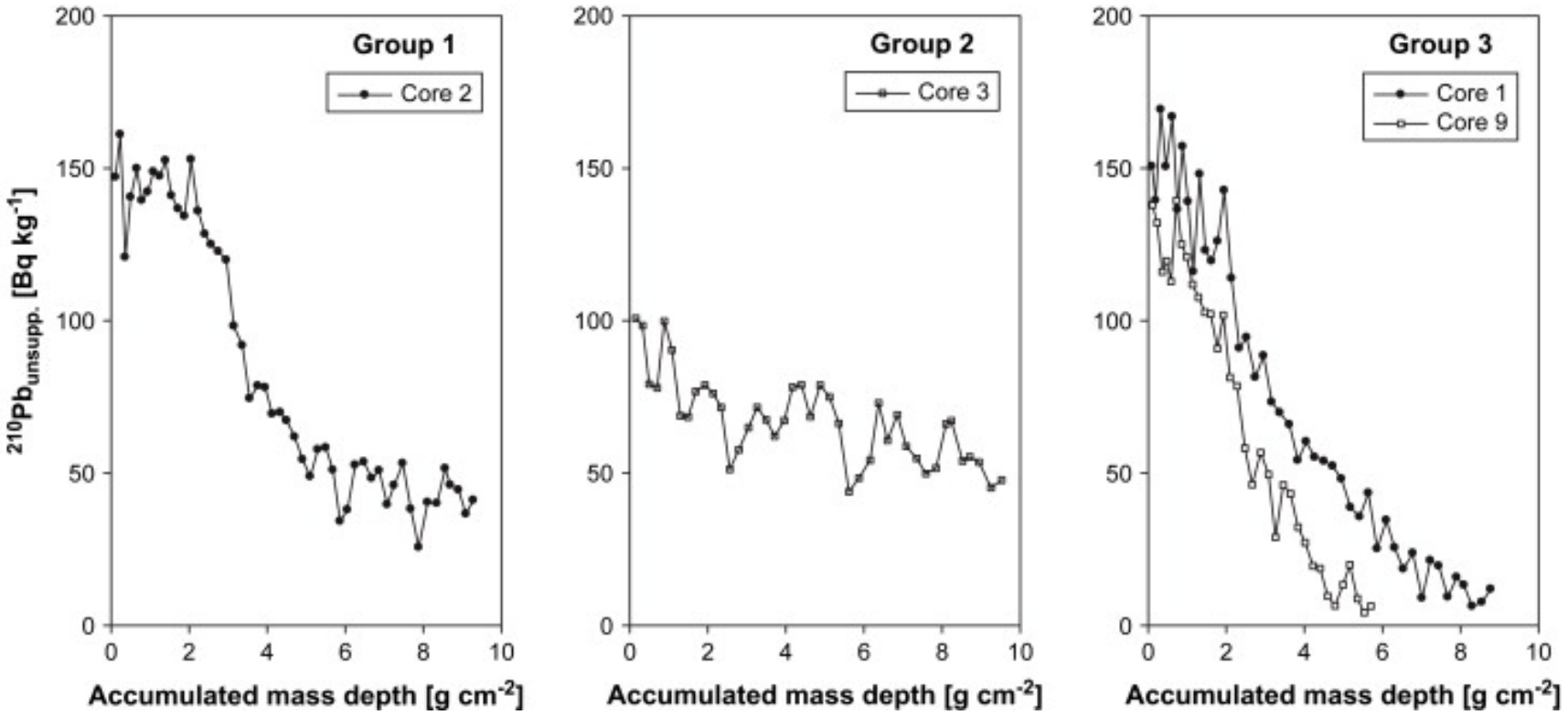

Fig. 6. Unsupported ^{210}Pb activity profile in sediment from maximum lake depth (group (1): core 2), debris fan in maximum lake depth (group (2): core 3); and intermediate lake depth levels (group (3): cores 1 and 9). Maximum uncertainty is <10%. t_o: 29th July 2004.